Research Article | Vol. 30, No. 2 / 17 Jan 2022 / Optics Express 1081

Optics EXPRESS

Generation of Huygens' dipoles for any spherical nanoparticle excited by counter-propagating plane waves: study of scattered helicity

L. CARRETERO,* P. ACEBAL, AND S. BLAYA

Universidad Miguel Hernández. Dpto. de Ciencia de Materiales, Óptica y Tecnología Electrónica, Avda. de la Universidad, 3202 Elche, Alicante, Spain

*l.carretero@umh.es

Abstract: Helicity and directionality control of scattered light by nanoparticles is an important task in different photonic fields. In this paper, we theoretically demonstrate that scattered light of lossy spherical nanoparticles excited by using two counter-propagating dephased plane waves with opposite helicity ± 1 and the adequate selection of dephase and intensity shows a well defined helicity and a controllable scattering directivity. Numerical examples of Si nanospheres are studied showing their potential application to directional nanoantennas with a well defined helicity. The proposed method is valid for any type of nanoparticle, not only lossy ones.

1. Introduction

The directionality control of scattered light by spherical nanoparticles and specially the intensity suppression at given directions were studied in an initial stage by Kerker and co-workers for non active particles [1], presenting Kerker's famous conditions and also those by Alexopoulos [2] and Kerker [3] for active objects. This directionality control of scattered light by spherical nanoparticles could have important applications, for example, in the field of nano-antennas [4,5] where generalization of Kerker's conditions have also been developed for nano-rings antennas [6]. Structured light beams have been used to obtain transverse Kerker scattering [7], which have been used to analyze nanoantenna displacements resolved with sub-angstrom precision and to achieve high scattering directivities in nanoantennas with radial and azimuthal polarization modes [8].

Kerker's conditions are related to duality symmetry of Maxwell equations [9], and consequently to conservation of electromagnetic helicity [10] that it is intimately linked with Noether's theorem [11,12].

When only one plane wave is used for illumination, second Kerker condition is precluded by the optical theorem for high refractive index particles in the absence of gain, while, as shown Olmos-Trigo et al. [13], the generalized second Kerker condition generates optimal backward scattering, but do not assures nearly-zero forward light scattering. Recently, it has been demonstrated by the same authors that nanoparticles with absorption or optical gain (active particles) preclude the first Kerker condition, and consequently, it is not possible to obtain zero backscattered radiation [14] and the scattered field don't have a well defined helicity when nanoparticles are illuminated by only one circularly polarized plane wave, so helicity is not preserved. This impossibility is due to the strict requirements that Mie coefficients must fulfil. In this sense, it has recently been demonstrated that control of light scattering can be obtained by means of the interference from multiple coherent waves for excitation of nanoparticles [15], where a TM mode is decomposed as a sum of different cylindrical waves. The simplest interference system can be obtained by using dephased counter-propagating linearly polarized plane waves, and these interference phenomena have been used to control the Mie scattering resonances [16],

#447827 https://doi.org/10.1364/OE.447827
Journal © 2022 Received 5 Nov 2021; revised 10 Dec 2021; accepted 10 Dec 2021; published 3 Jan 2022

Optics EXPRESS

which can be reduced or enhanced as a function of the relative phase of the waves. The approach used in this paper allows us to demonstrate that using dephased counter-propagating plane waves circularly polarized to excite nanoparticles (see Fig. 1) makes it possible for electric and magnetic modes simultaneously oscillate in-phase with equal amplitude, obtaining scattered fields with well defined helicity ±1 and enabling us to control the directionality of the scattering differential cross section by an adequate selection of dephase and amplitude ratio of counter-propagating plane waves.

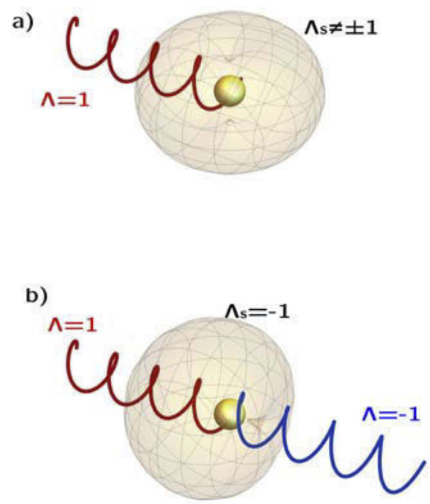

Fig. 1. (a) Non directional scattered field with helicity $\Lambda_s \neq \pm 1$ by an spherical nanoparticle excited by an incident plane wave with helicity 1. b) Backward scattered field with helicity $\Lambda_s = -1$ by an spherical nanoparticle excited by an two counter-propagating incident plane waves with helicities ±1 respectively.

2. Theoretical background

Let's consider two circularly polarized counter-propagating plane waves (see Fig. 1) along the Z axis (incident on a spherical particle of radius a, located at the coordinates' origin) whose electric and magnetic fields are given by:

$$\mathbf{E}_1 = E_0 exp(i\,k\,z)(\hat{x} + i\,\xi\hat{y}) \tag{1}$$

$$\mathbf{E}_2 = -E_0\,q\,exp\,(-i(\,k\,z - \delta)))\,(\hat{x} + i\,\xi\hat{y}) \tag{2}$$

$$\mathbf{H}_1 = \frac{1}{i\omega\mu}\nabla \times \mathbf{E}_1 \tag{3}$$

$$\mathbf{H}_2 = \frac{1}{i\omega\mu}\nabla \times \mathbf{E}_2 \tag{4}$$

resulting in a total electromagnetic incident field:

$$\mathbf{E}_i = \mathbf{E}_1 + \mathbf{E}_2 \tag{5}$$

$$\mathbf{H}_i = \mathbf{H}_1 + \mathbf{H}_2 \tag{6}$$

where E_0 is the amplitude of the incident electric field, q the beam ratio between amplitudes of the counter-propagating waves, δ is the dephase of counter-propagating plane waves and

$k^2 = \omega^2 \epsilon \mu$ is the appropriate wave number to the surrounding medium. A time dependence of $exp(-i\,\omega\, t)$ is assumed for all fields ω being the angular frequency. Using the Bohren notation [17], and generalizing (see Supplement 1) the results obtained by Li [16] for linearly polarized counter-propagating plane waves to circularly polarized counter-propagating plane waves given by Eqs. (1)–(4), we obtain scattered electric $\mathbf{E}_s$ and magnetic $\mathbf{H}_s$ fields induced by the spherical particle that can be expanded in vector spherical harmonics as:

$$\mathbf{E}_s = \sum_{n=1}^{\infty} E_n \left(i\,A_n\,\mathbf{N}^{(3)}_{e1n} - B_n\,\mathbf{M}^{(3)}_{o1n} + i\left(i\,A_n\,\mathbf{N}^{(3)}_{o1n} + B_n \mathbf{M}^{(3)}_{e1n} \right) \right) \tag{7}$$

$$\mathbf{H}_s = \frac{k}{\omega\mu} \sum_{n=1}^{\infty} E_n \left(A_n\,\mathbf{M}^{(3)}_{e1n} + i\,B_n\,\mathbf{N}^{(3)}_{o1n} + i\left(A_n\,\mathbf{M}^{(3)}_{o1n} - i\,B_n \mathbf{N}^{(3)}_{e1n} \right) \right) \tag{8}$$

where $E_n = E_0\, i^n\, \frac{2n+1}{n(n+1)}$, $\mathbf{N}^{(3)}_{e,o1n}, \mathbf{M}^{(3)}_{e,o1n}$ are the vector spherical harmonics [17], A_n and B_n being the parameters related to Mie coefficients a_n, b_n [17] by equations (see Supplement 1):

$$A_n = \left(1 + (-1)^n q\, exp(i\delta)\right) a_n \tag{9}$$

$$B_n = \left(1 - (-1)^n q\, exp(i\delta)\right) b_n \tag{10}$$

Note that if $q = 0 \implies A_n = a_n$, $B_n = b_n$, then Eqs. (7)–(10) represent the scattered field by a spherical particle generated by a circularly polarized incident plane wave, so A_n and B_n can be considered a generalization of Mie coefficients of the scattered field generated by two counter-propagating plane waves described by $\mathbf{E}_1$ and $\mathbf{E}_2$. These generalized Mie coefficients depend on the particles' geometry, refractive index, beam ratio, and the relative phase of the incident fields.

2.1. Directionality of scattered fields

In order to analyze the scattering directionality, we introduce the differential scattering cross sections that can be obtained as [14,17]:

$$\frac{d\sigma_s}{d\Omega}(\theta, \phi) = \lim_{r\to\infty} \frac{r^2 S_r}{S_i} \tag{11}$$

where S_r is the radial component of the Poynting vector $\mathbf{S} = \frac{1}{2}\Re[\mathbf{E}_s \times \mathbf{H}_s^*]$ and $S_i = |\mathbf{S}_1| + |\mathbf{S}_2|$, $\mathbf{S}_1$ and $\mathbf{S}_2$ being the Poynting vectors associated to the counter-propagating incident plane waves.

Thus, by using Eqs. (7) and (8), we introduce the directional scattering cross sections σ_b and σ_f as the differential scattering cross sections obtained at directions $\theta = 0$ and $\theta = \pi$:

$$\sigma_b = \frac{d\sigma_s}{d\Omega}(\pi, \phi) = \frac{1}{4k^2} \left| \sum_{n=1}^{\infty} (-1)^n (2n+1)(A_n - B_n) \right|^2 \tag{12}$$

$$\sigma_f = \frac{d\sigma_s}{d\Omega}(0, \phi) = \frac{1}{4k^2} \left| \sum_{n=1}^{\infty} (2n+1)(A_n + B_n) \right|^2 \tag{13}$$

It is important to note that σ_b and σ_f coincides to the backward and forward differential scattering cross sections when there is only one plane wave ($q = 0$) and then $A_n = a_n$ and $B_n = b_n$. It can be deduced that $\sigma_b = 0$ if $A_n = B_n$ whereas $\sigma_f = 0$ condition is accomplished when $A_n = -B_n$.

2.2. Helicity of scattered fields

On the other hand, the eigenstates of helicity operator $\Lambda = \frac{\nabla\times}{k}$ are given by the Riemann-Silberstein linear combination [18]:

$$\mathbf{G}_{\pm} = \frac{1}{\sqrt{2}}(\mathbf{E}_s \pm i\eta\mathbf{H}_s) \tag{14}$$

with $\eta = \sqrt{\mu/\epsilon}$ the medium impedance, so that:

$$\Lambda\mathbf{G}_{\pm} = \pm\mathbf{G}_{\pm} \tag{15}$$

which implies that $\mathbf{G}_{\pm}$ has a well defined helicity of ± 1.

By introducing (7) and (8) into Eq. (14), we obtain:

$$\mathbf{G}_{+}^{s} = \frac{i}{\sqrt{2}}\sum_{n=1}^{\infty} E_n(A_n + B_n)\left(\mathbf{M}_{e1n}^{(3)} + i\mathbf{M}_{o1n}^{(3)} + \mathbf{N}_{e1n}^{(3)} + i\mathbf{N}_{o1n}^{(3)}\right) \tag{16}$$

$$\mathbf{G}_{-}^{s} = \frac{1}{\sqrt{2}}\sum_{n=1}^{\infty} E_n(A_n - B_n)\left(-i\mathbf{M}_{e1n}^{(3)} + \mathbf{M}_{o1n}^{(3)} + i\mathbf{N}_{e1n}^{(3)} - \mathbf{N}_{o1n}^{(3)}\right) \tag{17}$$

By analyzing Eqs. (12), (13), (16) and (17) it can be deduced that if helicity of scattered fields is well defined with value +1, $\mathbf{G}_{-}^{s} = 0$ then $\sigma_b = 0$, and consequently, there is no scattering in the region z<-a; on the other hand, if the scattered helicity value is -1 then $\mathbf{G}_{+}^{s} = 0$, $\sigma_f = 0$ and there is no scattering in the region z>a. It is important to remark that it is not possible to obtain this result if linearly polarized incident waves are used, as we have demonstrated in Supplement 1.

Taking into account Eqs. (9) and (10), it can be deduced that if q=0, (no counter-propagating wave), the conditions $A_n = \pm B_n \implies a_n = \pm b_n$ corresponding to the well-known result whereby, at first and second Kerker conditions, the scattered field of a circularly polarized plane wave by a spherical nanoparticle shows a well defined helicity [19].

In this sense, an important result has recently been demonstrated affirming that either losses or optical gain inhibit the appearance of the first Kerker condition with one plane wave, so, $a_n \neq b_n, \forall n$. This result is due to the fact that the electric and magnetic modes cannot simultaneously oscillate in-phase with equal amplitude [14]. Furthermore, the authors have also shown that when the first Kerker condition is obtainable the second one is unreachable, so in real conditions, which generally imply losses, it is not possible to obtain the scattered field with a well defined helicity using only one incident beam, thus, zero optical backward or forward scattering is not reachable.

However, when counter propagating plane waves are used, the conditions necessary to obtain a well defined helicity in the scattered field is $A_n = \pm B_n$, and according to Eqs. (12) and (13), the scattered field will possess a directive radiation pattern with $\sigma_f = 0$ or $\sigma_b = 0$. It is important to note that the condition $A_n = \pm B_n$ implies that using suitable counterpropagating plane waves it is possible to achieve that electric and magnetic modes oscillate in phase or with a dephase π with equal amplitude, resulting a scattered field with well defined helicity and null scattering at the regions $z>a$ or $z<-a$, this result resembles the first and second Kerker conditions when there is only one plane wave.

If equation $A_n = \pm B_n$ is solved by taking into account Eqs. (9)– (10), thus we obtain the dephase parameter which is:

$$\delta = -i\,Log\left[\frac{(-1)^{1-n}(a_n \mp b_n)}{(a_n \pm b_n)q}\right] \tag{18}$$

so by definition, δ is a real number, then, the argument of the previous Log function must have module 1, so, the beam ratio q must be:

$$q = \left|\frac{(a_n \mp b_n)}{(a_n \pm b_n)}\right| \tag{19}$$

Introducing Eq. (18) into Eqs. (9)–(10) we obtain:

$$A_n = \frac{\pm 2a_n b_n}{a_n \pm b_n}; B_n = \frac{2a_n b_n}{a_n \pm b_n} \tag{20}$$

so although condition $a_n = \pm b_n$ is forbidden for real conditions, which generally imply losses and no gain [14], it is possible to obtain $A_n = \pm B_n$ by using an adequate dephase and beam ratio between counter-propagating plane waves

2.3. Dipolar approximation

With respect to the dipolar case ($n = 1$), Eq. (18) becomes:

$$\delta = -i\, Log\left[\frac{(a_1 \mp b_1)}{(a_1 \pm b_1)q}\right] \tag{21}$$

and Eq. (19) can be written as:

$$q = \left|\frac{a_1 \mp b_1}{(a_1 \pm b_1)}\right| = \frac{\sqrt{|a_1|^2 + |b_1|^2 \mp 2|a_1||b_1|cos(\Delta)}}{\sqrt{|a_1|^2 + |b_1|^2 \pm 2|a_1||b_1|cos(\Delta)}} \tag{22}$$

Introducing Eq. (22) into (21), we obtain:

$$\delta = arg\left[\frac{(a_1 \mp b_1)}{(a_1 \pm b_1)}\right] = arctan\left(\pm\frac{2|a_1||b_1|sin(\Delta)}{|a_1|^2 - |b_1|^2}\right) \tag{23}$$

where $\Delta = \phi_a - \phi_b$ being $\phi_a = arg(a_1)$ and $\phi_b = arg(b_1)$. Equations (22)–(23) constitute the main results of this paper, because they establish the relation between the nanoparticle's properties and the dephase and beam ratio parameter of the second plane wave that permits obtaining a scattered field with well defined helicity ±1 and $\sigma_f = 0$ or $\sigma_b = 0$ for any kind of material and wavelength.

An interesting result is the one obtained by taking the beam ratio $q = 1$ at Eq. (22), which results in $cos(\Delta) = 0$. This relation implies that $\Delta = \pm\pi/2$, a condition which would correspond to a Janus dipole [20], [21] when one plane wave illuminates the nanoparticle. Thus, these dipoles, illuminated by means of two counter-propagating plane waves given by Eq. (5), generate a scattered field that shows a well defined helicity ±1 if dephase parameter δ is adequately selected according to Eqs. (22)–(23), δ being in that case (see Supplement 1):

$$\delta_\pm = \pm 2\, arctan\left(\frac{|b_1|}{|a_1|}\right) \tag{24}$$

Let us assume the particular dipole obtained by taking $q = 1$ and $\Delta = -\pi/2$. In this case, σ_f and σ_b cross section can be obtained by introducing the dephase (24) into Eqs. (9),(10),(12) and (13), which results in:

$$\sigma_1 = \sigma_f(\delta_-) = \sigma_b(\delta_+) = \frac{18|a_1|^2|b_1|^2}{(|a_1|^2 + |b_1|^2)k^2} \tag{25}$$

When the same nanoparticle ($\Delta = -\pi/2$) is excited by using only one plane wave ($q = 0$), we have:

$$\sigma_0 = \sigma_f = \sigma_b = \frac{9(|a_1|^2 + |b_1|^2)}{4k^2} \tag{26}$$

From the last equations, it is clear that the directional scattering cross section obtained by using two plane waves is greater than that obtained using only a plane wave ($\sigma_1 > \sigma_0$), if the following condition is accomplished:

$$\frac{8|a_1|^2|b_1|^2}{(|a_1|^2+|b_1|^2)^2}>1 \implies (\sqrt{2}-1)<\frac{|a_1|}{|b_1|}<(\sqrt{2}+1) \tag{27}$$

Taking into account Eq. (11), the differential scattering cross section for these analyzed cases when $q = 1$ is given by:

$$\frac{d\sigma_{s1}}{d\Omega}(\delta_-) = \sigma_1 cos(\theta/2)^4 \tag{28}$$

$$\frac{d\sigma_{s1}}{d\Omega}(\delta_+) = \sigma_1 sin(\theta/2)^4 \tag{29}$$

and when $q = 0$:

$$\frac{d\sigma_{s0}}{d\Omega} = \frac{1}{4}\sigma_0\Big(3 + sin(2\theta)\Big) \tag{30}$$

2.4. Numerical results

In order to analyze the theoretical results shown above, Fig. 2 (a) illustrates the contour plot curves of Si spherical nanoparticles that present a phase difference between a_1 and b_1 of $-\pi/2$. As can be observed, there are many different sizes and wavelengths where nanoparticles show significant values of the imaginary part of the refractive index (absorption) where the first Kerker condition will be inhibited due to losses and the second Kerker condition will only be possible if the particle is pumped in order to obtain optical gain [14].

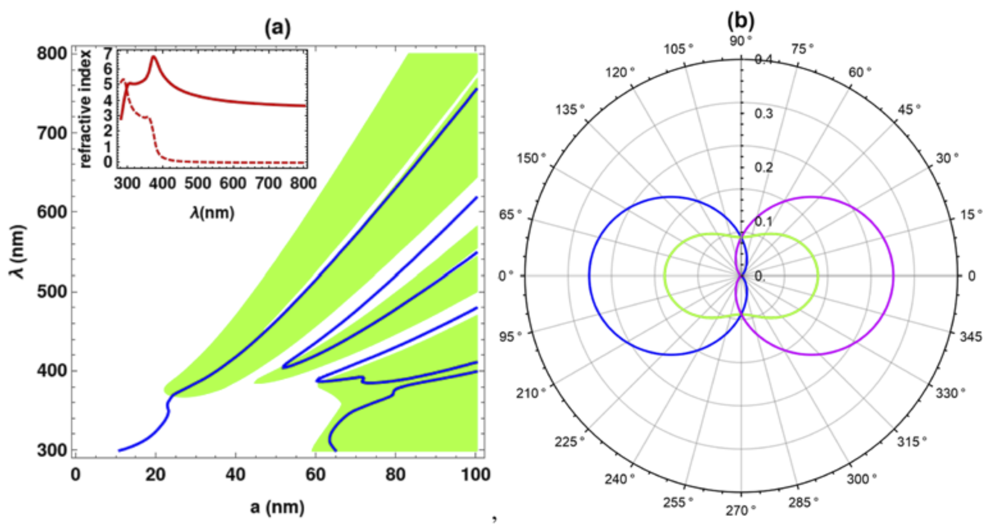

,

Fig. 2. (a) Contour plot curves showing the condition $(\phi_a - \phi_b) = -\pi/2$ as a function of particle radius a and wavelength λ for and Si nanoparticles, the inset graphics show the refractive index [22] Si nanoparticles (continuous red line corresponds to the real part and dashed to the imaginary part). Green plot region shows the radius and wavelengths that fullfill the inequality (27) for Si nanospheres. (b) Differential scattering cross section given by Eqs. (28)–(30) for Si nanoparticles illuminated by counterpropagating plane waves of beam ratio $q = 1$ (blue ($\delta = -1.658$) , magenta ($\delta = 1.658$)) and only one plane wave $q = 0$ (green).

In order to analyze the far-field radiation pattern behaviour of these dipoles, Fig. 2(b) shows the polar-plot of the differential scattering cross section given by Eqs. (28)–(30), which have azimuthal symmetry. To do this, by using the results shown in Fig. 2 (a), we studied the case

Si when nanoparticle has a radius $a = 30$ nm and it is illuminated by using a wavelength of 385.5 nm at which the refractive index is $6.28 + i0.65$. For this refractive index values, first and second Kerker conditions are forbidden [14], but in Fig. 2(b), it can be observed that null values of directional scattering cross sections σ_f and σ_b can be obtained for Si nanoparticles if the dephase parameter is selected according to Eq. (24). In the example, the dephase it is $\delta = \pm 1.658$. It is important to note that the directional scattering cross section is greater for the dipoles when two counter-propagating waves are used ($q = 1$) than when only one wave is used ($q = 0$) since the selected examples fulfil condition (27) an it is located in the green region of Fig. 2(a). Furthermore, the scattered field in Fig. 2(b) has a well defined helicity of ± 1 which can never be obtained by using only one illuminating plane wave. These results are essentially possible because of the adequate parameter's selection of the second illuminating plane wave, which permits obtaining electromagnetic modes that simultaneously oscillate in-phase with equal amplitude.

3. Conclusion

We have theoretically and numerically demonstrated that by exciting spherical nanoparticles with two circularly polarized counter-propagating plane waves, it is possible to obtain well defined helicity ± 1 for the scattered fields selecting the adequate dephase and beam ratio between incident fields. This is possible because by using the proposed method, electric and magnetic modes of nanoparticle simultaneously oscillate in-phase with equal amplitude obtaining a Huygens' dipole for any kind of material and wavelength. We have also shown that the scattered directivity of the particles illuminated by means of two plane waves can be higher that that obtained by using only one. The interferometric method proposed for lossy nanospheres can also be applied to active and non absorptive nanoparticles namely any type of material. These results can be applied to the design of directional nano-antennas.

Disclosures. The authors declare no conflicts of interest.

Data availability. No data were generated or analyzed in the presented research.

Supplemental document. See Supplement 1 for supporting content.

References

1. M. Kerker, D.-S. Wang, and C. L. Giles, "Electromagnetic scattering by magnetic spheres," J. Opt. Soc. Am. **73**(6), 765–767 (1983).
2. N. G. Alexopoulos and N. K. Uzunoglu, "Electromagnetic scattering from active objects: invisible scatterers," Appl. Opt. **17**(2), 235–239 (1978).
3. M. Kerker, "Electromagnetic scattering from active objects," Appl. Opt. **17**(21), 3337–3339 (1978).
4. N. Li, Y. Lai, S. H. Lam, H. Bai, L. Shao, and J. Wang, "Directional control of light with nanoantennas," Adv. Opt. Mater. **9**(1), 2001081 (2021).
5. Y. H. Fu, A. I. Kuznetsov, A. E. Miroshnichenko, Y. F. Yu, and B. Lukâyanchuk, "Directional visible light scattering by silicon nanoparticles," Nat. Commun. **4**(1), 1527 (2013).
6. R. Alaee, R. Filter, D. Lehr, F. Lederer, and C. Rockstuhl, "A generalized kerker condition for highly directive nanoantennas," Opt. Lett. **40**(11), 2645–2648 (2015).
7. A. Bag, M. Neugebauer, P. Woźniak, G. Leuchs, and P. Banzer, "Transverse kerker scattering for angstrom localization of nanoparticles," Phys. Rev. Lett. **121**(19), 193902 (2018).
8. S. Nechayev, J. S. Eismann, M. Neugebauer, P. Woźniak, A. Bag, G. Leuchs, and P. Banzer, "Huygens' dipole for polarization-controlled nanoscale light routing," Phys. Rev. A **99**(4), 041801 (2019).
9. X. Zambrana-Puyalto, I. Fernandez-Corbaton, M. L. Juan, X. Vidal, and G. Molina-Terriza, "Duality symmetry and kerker conditions," Opt. Lett. **38**(11), 1857–1859 (2013).
10. K. Y. Bliokh, A. Y. Bekshaev, and F. Nori, "Dual electromagnetism: helicity, spin, momentum and angular momentum," New J. Phys. **15**(3), 033026 (2013).
11. T. G. Philbin, "Lipkin's conservation law, noether's theorem, and the relation to optical helicity," Phys. Rev. A **87**(4), 043843 (2013).
12. R. P. Cameron and S. M. Barnett, "Electric–magnetic symmetry and noether's theorem," New J. Phys. **14**(12), 123019 (2012).
13. J. Olmos-Trigo, D. R. Abujetas, C. Sanz-Fernández, J. A. Sánchez-Gil, and J. J. Sáenz, "Optimal backward light scattering by dipolar particles," Phys. Rev. Research **2**(1), 013225 (2020).

Optics EXPRESS

14. J. Olmos-Trigo, C. Sanz-Fernández, D. R. Abujetas, J. Lasa-Alonso, N. de Sousa, A. García-Etxarri, J. A. Sánchez-Gil, G. Molina-Terriza, and J. J. Sáenz, "Kerker conditions upon lossless, absorption, and optical gain regimes," Phys. Rev. Lett. **125**(7), 073205 (2020).
15. J. Y. Lee, Y.-H. Chung, A. E. Miroshnichenko, and R.-K. Lee, "Linear control of light scattering with multiple coherent waves excitation," Opt. Lett. **44**(21), 5310–5313 (2019).
16. J. Li and P. Chýlek, "Resonances of a dielectric sphere illuminated by two counterpropagating plane waves," J. Opt. Soc. Am. A **10**(4), 687–692 (1993).
17. C. F.Bohren and D. Huffman, *Absorption and Scattering of Light by Small Particles* (Jonh Wiley & Sons, 1998).
18. I. Fernandez-Corbaton, M. Fruhnert, and C. Rockstuhl, "Objects of maximum electromagnetic chirality," Phys. Rev. X **6**, 031013 (2016).
19. I. Fernandez-Corbaton, Helicity and duality symmetry in light matter interactions: Theory and applications, https://arxiv.org/abs/1407.4432 (2015).
20. M. F. Picardi, M. Neugebauer, J. S. Eismann, G. Leuchs, P. Banzer, F. J. Rodríguez-Fortuño, and A. V. Zayats, "Experimental demonstration of linear and spinning janus dipoles for polarisation- and wavelength-selective near-field coupling," Light Sci Appl **8**(1), 52 (2019).
21. M. F. Picardi, A. V. Zayats, and F. J. Rodríguez-Fortuño, "Janus and huygens dipoles: Near-field directionality beyond spin-momentum locking," Phys. Rev. Lett. **120**(11), 117402 (2018).
22. M. N. Polyanskiy, Refractive index database, https://refractiveindex.info. Accessed on 2021-07-26.